Available online at www.sciencedirect.com
SCIENCE DIRECT®
Polyhedron 24 (2005) 1221–1231
POLYHEDRON
www.elsevier.com/locate/poly

X-ray diffraction, spectral and magnetic studies of the nickel(II) thiocyanate complexes with tridentate 2,6-dithiocarboxamidopyridine *SNS* and 2,6-dicarboxamidopyridine *ONO* ligands: Influence of donor atoms on the coordination geometry of nickel

Ramesh Kapoor [a,*], Ashok Kataria [a], Anuradha Pathak [a], Paloth Venugopalan [a], Geeta Hundal [b], Pratibha Kapoor [a]

[a] *Department of Chemistry, Panjab University, Chandigarh 160014, India*
[b] *Department of Chemistry, Guru Nanak Dev University, Amritsar 143005, India*

Received 1 February 2005; accepted 14 April 2005
Available online 31 May 2005

Abstract

The systematic investigation of electronic effects on the coordination geometry of nickel(II) thiocyanate complexes with the tridentate *N*,*N*,*N*′,*N*′-tetraethylpyridine-2,6-dithiocarboxamide (S-dept) and *N*,*N*,*N*′,*N*′-tetraethylpyridine-2,6-dicarboxamide (O-deap) ligands shows a significant change in the geometry of the metallic site. Their complexes conform to composition $[Ni_2(\mu\text{-}NCS)_2(S\text{-}dept)_2(NCS)_2]$ (**1**), $[Ni(NCS)_2(O\text{-}deap)(CH_3CN)] \cdot CH_3CN$ (**2**) and $[Ni(NCS)_2(O\text{-}deap)(C_2H_5OH)]$ (**3**), respectively. X-ray crystallographic studies were done for **1**–**3**. In the crystal lattice, complex **1** exists as a centrosymmetric dimer in which the dinuclear core is bridged by two N-bonded thiocyanate groups. The near octahedral geometry of the nickel atom is achieved through the two bridging N atoms of the thiocyanate groups, three *SNS* donor atoms of the ligand S-dept and through the terminal nitrogen atom of a non-bridging thiocyanate moiety. To the best of our knowledge, complex **1** presents the first example in literature with the highest asymmetry in N-bridging thiocyanato ligands. Ni ion is coordinated to *ONO* donor set of atoms of O-deap and two N-bonded NCS terminal groups. The sixth coordination site is completed by the N atom of an acetonitrile molecule. The coordination around Ni atom in **3** is also distorted octahedral. The change in the sixth coordination position from acetonitrile in **2** to ethanol in **3** has a profound influence in the overall topology of the metal–ligand complex. The complex interplay of weak interactions in stabilizing the 3-dimensional lattice of these molecules is well demonstrated.

Keywords: Nickel(II) thiocyanate; *N*,*N*,*N*′,*N*′-tetraethylpyridine-2,6-dithiocarboxamide (S-dept); *N*,*N*,*N*′,*N*′-tetraethylpyridine-2,6-dicarboxamide (O-deap); Centrosymmetric

1. Introduction

Over the past few years, there has been a growing interest in the development of coordination chemistry of tridentate 2,6-dicarboxamidopyridine ligands toward transition metal [1–5] and lanthanide ions [6]. Most of these studies have been focussed on recognising the strong donor capacity of the deprotonated pyridine-2,6-dicarboxamide moiety in transition metal complexes [1–4]. Recently, we [7] and others [6,8,9] have developed a number of tridentate ligands based on the fully substituted pyridine-2,6-dicarboxamide moiety. Our interest

* Corresponding author. Tel.: +91 172 254 1435; fax: +91 172 254 5074.
E-mail address: rkapoor@pu.ac.in (R. Kapoor).

0277-5387/$ - see front matter © 2005 Elsevier Ltd. All rights reserved.
doi:10.1016/j.poly.2005.04.006

in the study of *N*,*N*,*N*′,*N*′-tetraalkylpyridine-2,6-dicarboxamide ligands has been twofold: firstly, to study the effect of steric congestion brought by employing isopropyl or phenyl groups at the terminal carboxamide side arms, i.e., R = $-CH(CH_3)_2$ or $-C_6H_5$ and secondly to investigate the effect of change in the donor set of atoms in the two side arms on the coordination geometry adopted by the complexes. In our recent studies, it has been shown that substitution of the donor atoms by atoms of different size and electronegativity is reflected by major changes in the coordination geometries and solid state structures adopted by the corresponding complexes [7]. Crystal structures of Cu_2Cl_4(S-dept) and $CuCl_2$(O-deap) have shown important differences between the two complexes. Cu_2Cl_4(S-dept) is a tetranuclear copper(II) complex, formed by a cationic $[Cu_2Cl_2\{\mu\text{-(S-dept)}\}_2]^{2+}$ and an anionic dinuclear complex $[Cu_2Cl_4(\mu\text{-}Cl)_2]^{2-}$ [7c]. On the other hand, $CuCl_2$(O-deap) is a five coordinated trigonally distorted rectangular pyramidal complex [7a]. Similarly, complexes of $CoCl_2$ with S-dept and O-deap have revealed different structures [7b]. This paper describes the comparative X-ray diffraction, IR and visible spectra and magnetic properties of the nickel(II) thiocyanate complexes of tridentate *SNS* and *ONO* donor ligands S-dept and O-deap. Stabilization of the metal–ligand complexes of O-deap in the solid state critically depends upon the solvent used for crystallization. The role of coordinating solvents like acetonitrile and ethanol in the lattice stabilization of the complex is discussed in the paper. It was also of interest to investigate the different thiocyanate bonding modes present in these complexes.

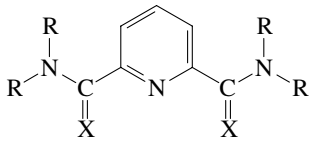

X=S; R= Et (S-dept)
X=O; R= Et (O-deap)

2. Experimental

2.1. Materials

All reactions were carried out in anhydrous solvents. Solvents were dried using standard techniques. Absolute ethanol (AR quality, Hayman Ltd.) and pyridine-2,6-dicarboxylic acid (Fluka) were used as supplied. Anhydrous $NiCl_2$ was prepared by boiling the hydrated salt under reflux with freshly distilled $SOCl_2$ for about 4 h. The anhydrous $NiCl_2$ was filtered, washed with dry benzene and dried in vacuo.

2.2. Preparation of *N*,*N*,*N*′,*N*′-tetraethylpyridine-2,6-dicarboxamide (O-deap) and *N*,*N*,*N*′,*N*′-tetraethylpyridine-2,6-dithiocarboxamide (S-dept)

O-deap was prepared as described earlier [5]. S-dept was obtained by refluxing a mixture of O-deap (8.26 g, 0.03 mol) and P_2S_5 (4.13 g, 0.018 mol) in benzene (50 mL) for 8 h. The reaction mixture was filtered to remove unreacted P_2S_5. Crude sample of S-dept was recovered by removal of the solvent under vacuum. Pure product was obtained as shinning yellow crystals on crystallization from hot ethanol (yield: 7.37 g, 80%). M.p. 130 °C. *Anal*. Calc. for $C_{15}H_{23}N_3S_2$: C, 58.25; H, 7.44; N, 13.59. Found: C, 58.10; H, 7.56; N, 13.48%.

2.3. Ni(S-dept)(NCS)$_2$ (**1**)

A solution of 3 mmol of anhydrous $NiCl_2$ in 20 mL of ethanol was added to a solution of 6 mmol of KSCN in 20 mL of ethanol. The filtrate after removal of quantitative amount of KCl was refluxed with 3 mmol of S-dept for 4 h. Dark brown precipitates of **1** separated out at room temperature. Recrystallization from ethanol gave dark-brown crystals. Yield: 1.26 g (87%); m.p. 226 °C. *Anal*. Calc. for $C_{34}H_{46}N_{10}S_8Ni_2$: C, 42.17; H, 4.75; N, 14.47; S, 26.5; Ni, 12.1. Found: C, 41.76; H, 5.03; N, 14.26; S, 26.1; Ni, 12.0%. Molar conductance [Λ_M, Ω cm^2 mol^{-1}]: 12.0 (CH_3CN) (expected range for 1:1 electrolytes: 120–160 Ω cm^2 mol^{-1}). IR (KBr pellet, cm^{-1}): 2087, 2007, 1602, 1581, 1518, 1469, 1450, 1388, 1360, 1316, 1282, 1260, 1186, 1145, 1094, 1017, 811, 722, 625, 474. Visible spectral data [λ_{max}, nm (ε, M^{-1} cm^{-1})] in methanol: 406 (265), 661 (8.1), 727 sh (6.5), 1092 (7.6). FAB mass [(*m*-nitrobenzyl alcohol): (M^+, 966)], *m*/*z*: 734 [Ni_2(S-dept)$_2$], 676 [Ni(S-dept)$_2$]$^+$, 425 [Ni_2(S-dept)]$^+$, 367 [Ni(S-dept)]$^+$ (base peak), 338 [Ni(S-dept)-C_2H_5]$^+$, 310 [Ni(S-dept)-C_2H_5-C_2H_4]$^+$, 278 [Ni(S-dept)-C_2H_5-C_2H_4-S]$^+$.

2.4. [Ni(NCS)$_2$(O-deap)(CH_3CN)] · CH_3CN (**2**)

This was prepared by the procedure adopted for **1**, except CH_3CN was used as the medium and O-deap as ligand. Recrystallization from acetonitrile gave green crystals. Yield: 1.47 g (91%); m.p. 220 °C. *Anal*. Calc. for $C_{21}H_{29}N_7O_2S_2Ni$: C, 47.19; H, 5.43; N, 18.35; S, 12.0; Ni, 11.0. Found: C, 47.58; H, 5.87; N, 17.97; S, 11.7; Ni, 10.7%. Molar conductance [Λ_M, Ω cm^2 mol^{-1}]: 18 (CH_3CN). IR (KBr pellet, cm^{-1}): 2315, 2287, 2092, 1600, 1561, 1315, 1270, 1198, 1098, 1069, 1046, 1030, 947, 829, 758, 723, 698, 656, 511, 447. Visible spectral data [λ_{max}, nm (ε, M^{-1} cm^{-1})] in methanol: 390 (13.1), 670 (1.7), 742 (1.9), 1071 (1.4).

2.5. [Ni(NCS)$_2$(O-deap)(C$_2$H$_5$OH)] (3)

This complex was prepared by the same procedure but anhydrous ethanol was used as the reaction medium. Yield: 1.20 g (90%); m.p. 200 °C. *Anal.* Calc. for $C_{19}H_{29}N_5O_3S_2Ni$: C, 45.78; H, 5.82; N, 14.05; S, 12.8; Ni, 11.8. Found: C, 45.24; H, 5.64; N, 14.02; S, 12.4; Ni, 11.3%. Molar conductance [Λ_M, Ω cm^2 mol^{-1}]: 6.0 (C_2H_5OH) (expected range for 1:1 electrolytes: 30–45 Ω cm^2 mol^{-1}). IR (KBr pellet, cm^{-1}): 3196, 2100, 1600, 1562, 1316, 1272, 1198, 1098, 1070, 1049, 1030, 947, 830, 762, 722, 705, 657, 510, 442. Visible spectral data [λ_{max}, nm (ε, M^{-1} cm^{-1})] in ethanol: 370 sh (14.2), 664 (4.4), 728 (4.5), 1080 (4.8).

2.6. Physical methods

Elemental analysis (C, H, N) were performed on a Perkin–Elmer Model 2400 CHN analyzer at RSIC, Panjab university, Chandigarh. IR spectra were recorded as Nujol/hcb mulls on KBr plates on a Perkin–Elmer RX-1 FTIR spectrophotometer. The UV–Vis spectra were recorded on a JASCO V-530 UV–Vis spectrophotometer. Reflectance spectra were recorded on an integrating sphere Hitachi model 330 using $MgCO_3$. The FAB mass spectra were recorded on a JEOL SX 102/DA-6000 Mass Spectrometer/Data System using Argon/Xenon (6 kV, 10 mA) as the FAB gas. *m*-Nitrobenzyl alcohol (NBA) was used as the matrix. Variable temperature (34–300 K)[1] solid state magnetic susceptibility measurements were done using a locally built Faraday balance [2].

2.7. X-ray crystallography

The crystals of complexes **1** and **3** were grown from ethanol and **2** from acetonitrile by a method of slow evaporation at room temperature. The data were collected on a Siemens P4 single crystal diffractometer using graphite monochromatized Mo Kα radiation (0.71073 Å). Table 1 shows the unit cell parameters and data measurement details. Data collection and cell refinement were done with XSCANS [10]. Data were corrected for Lorentz and polarization effects but no absorption correction was performed for **1**. Structure was solved by direct methods and refined anisotropically by full matrix least squares methods. All the hydrogens were fixed geometrically as riding atoms with a displacement parameter equal to 1.2 (CH, CH_2) or 1.5 (CH_3) times that of the parent atoms. Data reduction, structure solutions, refinement and molecular graphics were performed using SHELXLTL-PC [11]. During refinement the terminal ethyl groups of the dithioamide ligand showed disorder in terms of abnormal bond lengths and high thermal parameters. The disorder could be resolved successfully for C8, C10, C13, C15 methyl and C9, C12 methylene carbon atoms. Each of their atomic positions was split into two peaks with a total site occupancy of 1.000. These atoms were refined isotropically with restraints using fixed C–C (1.510 Å) and C–N (1.456 Å) distances. All other atoms were refined anisotropically. Torsion angles and least squares planes were calculated by using PARST [12]. The data collection procedure,structure solution and refinement for **2** and **3** were as follows, **2**: 40 reflections ($9.685° < 2\theta < 29.236°$) for accurate cell parameter determination, a total of 26.56 h of X-ray exposure time, $R = 0.0307$, $wR = 0.0780$, $a = 0.0471$ and $b = 0.22$ [in the weighting scheme]. **3**: 40 reflections ($10.207° < 2\theta < 29.936°$) for accurate cell parameter determination, a total of 39.65 h of X-ray exposure time, $R = 0.0465$, $wR = 0.1178$, $a = 0.0627$ and $b = 7.53$ [in the weighting scheme]. CCDC numbers for the complexes **1**, **2** and **3** are 261983, 261984 and 261985, respectively.

3. Results and discussion

Complexes **1**–**3** were obtained in good yield by refluxing $Ni(NCS)_2$ and the S-dept or O-deap ligand. These complexes are air and moisture stable and readily dissolved in common organic solvents. Conductance values in CH_3CN and C_2H_5OH did not show dissociation into ionic species [13]. No molecular ion peak corresponding to the dinuclear nickel species [{Ni(S-dept)(SCN)$_2$}$_2$] (*m*/*z*, 966) was observed in the FAB mass spectrum of **1**. However, some structurally important nickel containing ions were observed (see Section 2). Instability of M^+ ion may be attributed to the facile loss of 2 moles of $(NCS)_2$; the driving force for the formation of [Ni$_2$(S-dept)$_2$] may be the formation of Ni–Ni bond. Thermal analysis (TGA) of complex **1** in air shows that the weight loss of 27.0% between 230 and 320 °C corresponds to the removal of $(SCN)_2$ and ethylene. On heating above 320 °C, it loses the entire organic mass to yield NiO. TGA of **2** did not show the formation of any stable intermediates. The complex on heating above 60 °C loses all the organic components to yield a stable residue of NiO at 680 °C. The μ_{eff} values at 300 K for **1, 2** and **3** (per Ni atom) are 2.98, 2.82 and 2.88 μ_B, respectively. The magnetic moment of **1** was measured over the temperature range 300–34 K[1] (Fig. 1). The $\chi_M T$ value is almost constant (2.205 cm^3 mol^{-1} K) in the range 300–200 K. Below this temperature, $\chi_M T$ decreases slowly to 2.006 cm^3 mol^{-1} K upto 100 K. Between 100 and 34 K, it decreases to 1.326 cm^3 mol^{-1} K. This behaviour suggests the presence of weak antiferromagnetic interactions. The equations for dimers with two $S = 1$ metal ions (as is the case for dinuclear Ni compounds) is

[1] Due to lack of facilities measurements could not be extended below 34 K.

Table 1
Crystal data and structure refinement for complexes **1**–**3**

Complex	**1**	**2**	**3**
Empirical formula	$C_{17}H_{23}N_5NiS_4$	$C_{21}H_{29}N_7NiO_2S_2$	$C_{19}H_{29}N_5NiO_3S_2$
Formula weight	484.35	534.34	498.30
T (K)	293(2)	293(2)	293(2)
Wavelength (Å)	0.71069	0.71073	0.71073
Crystal system	monoclinic	monoclinic	monoclinic
Space group	$P2_1/c$	$P2_1$	$C2/c$
Unit cell dimensions			
a (Å)	9.623(5)	8.327(1)	29.33(2)
b (Å)	14.361(5)	10.909(1)	13.286(1)
c (Å)	16.284(5)	15.136(1)	15.877(1)
α (°)	90.0	90	90
β (°)	95.4(5)	97.91(1)	121.63(1)
γ (°)	90.0	90	90
V (Å^3)	2240.4(16)	1361.9(2)	5267.9(6)
Z	4	2	8
D_{calc} (Mg/m^3)	1.436	1.303	1.257
Absorption coefficient (mm^{-1})	1.251	0.895	0.921
F(000)	1008	560	2096
Crystal size (mm)	$0.15 \times 0.12 \times 0.10$	$0.21 \times 0.19 \times 0.16$	$0.27 \times 0.24 \times 0.17$
θ Range for data collection (°)	1.89–27.50	2.31–24.01	2.00–24.00
Scan type	2θ–θ	2θ–θ	2θ–θ
Scan speed	variable, 2.0–60.0°/min in ω	variable, 2.0–60.0°/min in ω	variable, 2.0–60.0°/min in ω
Limiting indices	$0 \leqslant h \leqslant 12$, $0 \leqslant k \leqslant 18$, $-21 \leqslant l \leqslant 21$	$0 \leqslant h \leqslant 9$, $0 \leqslant k \leqslant 12$, $-17 \leqslant l \leqslant 17$	$0 \leqslant h \leqslant 33$, $0 \leqslant k \leqslant 15$, $-18 \leqslant l \leqslant 15$
Reflections collected/unique (R_{int})	5456/5152 (0.0691)	2447/2276 (0.0182)	4232/4144 (0.0147)
Refinement method	full-matrix least-squares on F^2	full-matrix least-squares on F^2	full-matrix least-squares on F^2
Data/restraints/parameters	5152/12/238	2276/1/299	4144/0/272
Goodness-of-fit on F^2	0.995	1.027	1.013
Final R indices [$I > 2\sigma(I)$]	$R_1 = 0.0900$, $wR_2 = 0.2015$	$R_1 = 0.0307$, $wR_2 = 0.0780$	$R_1 = 0.0465$, $wR_2 = 0.1178$
R indices (all data)	$R_1 = 0.2189$, $wR_2 = 0.2727$	$R_1 = 0.0344$, $wR_2 = 0.0803$	$R_1 = 0.0654$, $wR_2 = 0.1262$
Largest difference in peak and hole (e Å^{-3})	0.991 and −0.717	0.225 and −0.243	0.763 and −0.523

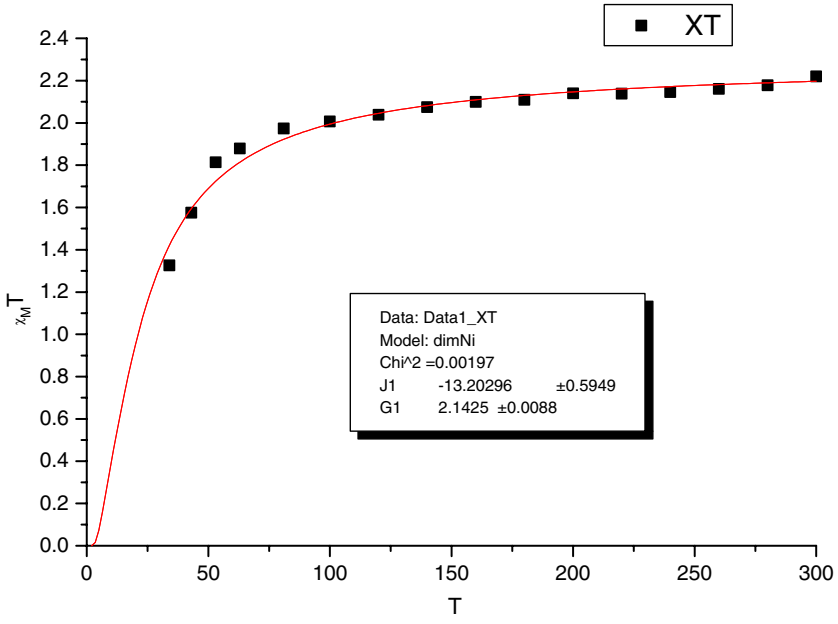

Fig. 1. Showing the variation of $\chi_M T$ with T for complex **1**.

derived from Van Vleck's equation and, by using the spin hamiltonian, $H = -JS_1 \times S_2$, it takes the following form: $\chi T = (Ng^2\beta^2/k)[(2\exp(x) + 10 \times \exp(3x))/(1 + 3\exp(x) + 5\exp(3x))]$, where $x = J/kT$, k being the Boltzman's constant, and J the magnetic coupling constant (in cm^{-1}). The results of the best fit, shown

as the solid line in Fig. 1, were $J = -13.203 \pm 0.595$ cm^{-1}, $g = 2.142 \pm 0.009$.

3.1. Spectroscopic properties

3.1.1. IR spectra

Complex **1** shows two distinct ν(CN) modes for the NCS^- group, at 2087 and 2007 cm^{-1}. The higher frequency band is assigned to the N-bonded terminal thiocyanate group [14], and the lower frequency band at 2007 cm^{-1} strongly indicates the presence of N-bridging thiocyanate ligand joining the two nickel centres. This unusual bridging mode of thiocyanate ligand has been observed for a very limited number of complexes which are listed in Table 3 [15–19]. The position of the C–S stretching frequency in the region 860–690 cm^{-1} is usually employed for differentiating S-bonded from N-bonded terminal thiocyanates [14,20]. However, the ν(CS) modes are obscured by ligand bands in this region which made assignment of the C–S stretches quite uncertain. The peaks attributed to ν(CN) are not perturbed in its solution spectrum thus suggesting that the solid state structure is retained in $CHCl_3$ solution. Complexes 2 and 3 show a single band in the ν(CN) region, at 2092 and 2100 cm^{-1}, respectively, which are assigned to the N-bonded terminal NCS ligands. The carbonyl stretching frequency which appears at 1625 cm^{-1} in the free ligand is shifted to 1600 cm^{-1} suggesting carbonyl coordination to metal centre.

3.1.2. Visible spectra

Complexes **1**–**3** show a close resemblance between absorption in methanol and their reflectance spectra suggesting that the same geometry is retained by the metal ion on dissolution. Complex **1** exhibits three distinct absorption bands at 406, 661 and 1090 with a shoulder band at 738 nm. Similar spectra are observed for **2** and **3**with bands at 390, 670 (sh), 742 and 1080 and 370 (sh), 664, 728 and 1080 nm, respectively. Assuming Oh symmetry for the Ni ions in these compounds, the bands may be assigned to the spin allowed d-d transitions $^3T_{1g}(P) \leftarrow {}^3A_{2g}$, $^3T_{1g}(F) \leftarrow {}^3A_{2g}$ and $^3T_{2g} \leftarrow {}^3A_{2g}$, respectively. The band at about 730 nm may be a consequence of the transition to the ^1E_g level gaining intensity through configurational interaction with the $^3T_{1g}(F)$ level.

3.2. Crystal structures of complexes *1*–*3*

3.2.1. Complex *1*

Crystallization of **1** from ethanol or acetonitrile by slow evaporation of its saturated solution at room temperature afforded good single crystals of $[Ni_2(\mu\text{-}NCS)_2(S\text{-}dept)_2(NCS)_2]$. The bond lengths and angles are listed in Table 2. The complex is a centrosymmetric dimer (Fig. 2). It consists of two distorted octahedrons, one about each Ni^{2+}, which share an edge, formed by the N atoms of the bridging NCS ions. The remaining sites are occupied by two S and one N atoms from the tridentate chelating ligand and from a N atom of the terminally bonded thiocyanate ion. The bond angles around Ni^{2+} are close to that of an ion in an octahedral environment. Both Ni–S bonds are equal and trans to each other. The three M–N bonds in the xy plane are equal with an average M–N distance of 2.028(7) Å. The four nitrogens N1 N4 N5 and $N4^i$ (where i = $-x$, $-y$, $-z + 1$) are almost planar with a deviation of 0.016 Å from a least square plane. The M–N bond lengths for the bridging NCS ligands are Ni–N4 2.022(7) and Ni–$N4^i$ 2.396(8) Å, respectively. This shows that NCS is behaving as an unsymmetrical bridging bidentate ligand through N. The bridging NCS ligands are perpendicular to Ni–Ni^i axis with Ni–N–Ni^i angle of 96.9° (**3**). Ni–Ni distance is 3.316(8) Å, which indicates the absence of any metal–metal bond. Both bridging and terminal NCS ligands are almost linear with small differences in their respective bond distances and angles. The bonding parameters of the terminal NCS ligand fall well within the range generally observed in the literature [15–19,21]. The short N–C distance [N(5)–C(17), 1.151(12) Å] corresponds with structure **I**. The C–S bond distance [C(17)–S(4), 1.631(12) Å] is shorter than the C–S(sp^3) bond distance (1.81 Å) but is close to C=S bond distance (1.61 Å) as given by Pauling [22]. However, it falls well within the range 1.588(13)–1.689(13) Å found for terminally bonded covalent NCS group. The terminal M–NCS linkages in this complex are bent with M–N–C angle 170.8° (8) which fall in the range (141–174°) found for Ni^{2+} having bent terminally bonded NCS anions [6b]. Ni–N5–C17–S4 torsion angle is 15.1°. This non-linearity has been attributed to the steric effects [23] and indicates more electron density localization on N so that **II** becomes the major contributing resonance structure for NCS anion [24].

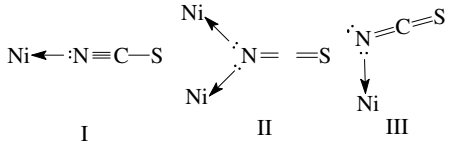

The C–S bond length [C(16)–S(3), 1.606(10) Å] of the bridging NCS ion is more closer to C=S and is in conformity with structure **II**. As already known [14] this also accounts for the two lone pairs on N atoms directed at the metal ion and the linearity of the group, however, N–C bond [N(4)–C(16), 1.145(10) Å] remains too short to be a double bond. This short N–C bond may be due to inductive effect, which results due to greater flow of electron density from the C–S bond through the C–N bond towards metal ion, as shown in **III**. Bridging through N requires M–NCS linkages to be essentially

Table 2
Important bond lengths (Å) and bond angles (°) for complexes **1**–**3**

Complex ***1***[a]	
Ni–N(5)	2.018(9)
Ni–N(4)	2.022(7)
Ni–N(1)	2.043(6)
Ni–S(2)	2.384(3)
Ni–S(1)	2.388(3)
Ni–(N4)^{i}	2.396(8)
S(1)–C(6)	1.651(9)
S(2)–C(11)	1.656(8)
S(3)–C(16)	1.606(10)
S(4)–C(17)	1.631(12)
N(4)–C(16)	1.145(10)
N(5)–C(17)	1.151(12)
N(5)–Ni–N(4)	95.7(3)
N(5)–Ni–N(1)	91.2(3)
N(4)–Ni–N(1)	173.0(3)
N(5)–Ni–S(2)	91.8(2)
N(4)–Ni–S(2)	95.8(2)
N(1)–Ni–S(2)	84.0(2)
N(5)–Ni–S(1)	93.9(2)
N(4)–Ni–S(1)	96.1(2)
C(16)–N(4)–Ni	149.2(8)
C(16)–N(4)–Ni^{i}	113.8(7)
N(1)–Ni–S(1)	83.3(2)
S(2)–Ni–S(1)	1666.19(10)
N(5)–Ni–N(4)^{i}	178.0(3)
N(4)–Ni–N(4)^{i}	83.1(3)
N(1)–Ni–N(4)^{i}	90.0(3)
S(2)–Ni–N(4)^{i}	86.79(19)
S(1)–Ni–N(4)^{i}	87.81(19)
Ni–N(4)–Ni^{i}	96.9(3)
C(17)–N(5)–Ni	170.8(8)
Complex ***2***	
Ni(1)–N(5)	1.995(3)
Ni(1)–N(6)	2.043(4)
Ni(1)–O(1)	2.098(4)
S(1)–C(18)	1.620(4)
O(1)–C(6)	1.252(5)
N(1)–C(5)	1.337(6)
N(2)–C(6)	1.341(6)
N(2)–C(7)	1.493(6)
N(3)–C(14)	1.470(6)
N(4)–C(16)	1.118(6)
N(6)–C(19)	1.146(7)
Ni(1)–N(1)	2.023(3)
Ni(1)–O(2)	2.085(3)
Ni(1)–N(4)	2.141(4)
S(2)–C(19)	1.632(6)
O(2)–C(11)	1.249(5)
N(1)–C(1)	1.347(6)
N(2)–C(9)	1.481(7)
N(3)–C(11)	1.331(5)
N(3)–C(12)	1.474(6)
N(5)–C(18)	1.155(4)
N(7)–C(20)	1.122(13)
N(5)–Ni(1)–N(1)	177.48(15)
N(1)–Ni(1)–N(6)	90.65(15)
N(1)–Ni(1)–O(2)	77.74(15)
N(5)–Ni(1)–O(1)	103.20(17)
N(6)–Ni(1)–O(1)	94.72(17)
N(5)–Ni(1)–N(4)	88.84(17)
N(6)–Ni(1)–N(4)	179.29(17)

Table 2 (*continued*)

Complex ***2***	
O(1)–Ni(1)–N(4)	84.84(16)
C(11)–O(2)–Ni(1)	114.5(2)
C(5)–N(1)–Ni(1)	117.6(3)
C(6)–N(2)–C(9)	116.8(4)
C(9)–N(2)–C(7)	115.5(4)
C(11)–N(3)–C(12)	126.8(4)
C(16)–N(4)–Ni(1)	177.5(4)
C(19)–N(6)–Ni(1)	162.7(4)
N(1)–C(1)–C(6)	110.1(3)
N(5)–Ni(1)–N(6)	91.81(17)
N(5)–Ni(1)–O(2)	101.63(16)
N(6)–Ni(1)–O(2)	91.00(16)
N(1)–Ni(1)–O(1)	77.16(16)
O(2)–Ni(1)–O(1)	154.30(11)
N(1)–Ni(1)–N(4)	88.71(15)
O(2)–Ni(1)–N(4)	89.16(15)
C(6)–O(1)–Ni(1)	115.7(3)
C(5)–N(1)–C(1)	122.3(3)
C(1)–N(1)–Ni(1)	118.5(3)
C(6)–N(2)–C(7)	127.5(4)
C(11)–N(3)–C(14)	117.2(3)
C(14)–N(3)–C(12)	115.8(4)
C(18)–N(5)–Ni(1)	178.0(5)
N(1)–C(1)–C(2)	119.8(4)
C(2)–C(1)–C(6)	129.9(4)
Complex ***3***	
Ni(1)–N(4)	1.980(3)
Ni(1)–N(5)	2.045(3)
Ni(1)–O(1)	2.123(2)
S(1)–C(16)	1.625(5)
O(1)–C(6)	1.256(4)
O(3)–C(18)	1.414(6)
Ni(1)–N(1)	2.030(3)
Ni(1)–O(3)	2.078(3)
NI(1)–O(2)	2.137(2)
S(2)–C(17)	1.634(4)
O(2)–C(11)	1.254(4)
N(4)–Ni(1)–N(1)	176.85(12)
N(1)–Ni(1)–N(5)	89.67(12)
N(1)–Ni(1)–O(3)	90.20(11)
N(4)–Ni(1)–O(1)	106.16(12)
N(5)–Ni(1)–O(1)	90.07(12)
N(4)–Ni(1)–O(2)	99.55(12)
N(5)–Ni(1)–O(2)	93.07(12)
O(1)–Ni(1)–O(2)	154.03(10)
C(11)–O(2)–Ni(1)	112.9(2)
C(1)–N(1)–Ni(1)	116.6(2)
N(4)–Ni(1)–N(5)	91.08(14)
N(4)–Ni(1)–O(3)	89.07(13)
N(5)–Ni(1)–O(3)	179.67(14)
N(1)–Ni(1)–O(1)	76.90(10)
O(3)–Ni(1)–O(1)	89.60(12)
N(1)–Ni(1)–O(2)	77.35(10)
O(3)–Ni(1)–O(2)	87.20(12)
C(6)–O(1)–Ni(1)	114.4(2)
C(18)–O(3)–Ni(1)	126.6(3)

[a] Symmetry i: $-x, -y, -z + 1$.

angular with M–N–C being 149.2(8)° and 113.8(7)°. The first example of an N-bonded NCS bridging ligand was reported for a mixed valence Re^{III}/Re^{IV} complex [15]. It

Table 3
Various bond lengths (Å) and bond angles (°) found in complexes of NCS anion having bidentate, N-bridging mode of coordination

S. no.	Complex	Type of bond	M–N	C–N	C–S	N–C–S	M–N–C	M–N–M	M–M
1	$[Re_2(NCS)_{10}]^{3-}$ (**2**)	terminal[a]	2.026(8)	1.16(1)	1.59(1)	178.8(9)	171.8(7)	77.4(3)	2.613(1)
		bridging[a]	2.087(8), 2.095(8)	1.17(1)	1.57(1)	178.7(8)	141.5(7)		
2	$[Cd_2(NCS)_4(butrz)_3]_n$ (**3**)	terminal[a]	2.240(3)					100.83(9)	3.6912(4)
		bridging[a]	2.352(3), 2.437(3)						
3	$Ni_3(detrH)_6(NCS)_6$ (**7**)	terminal[a]	2.04(1)	1.15(1)	1.64(1)	177.4(9)	163.3(9)	105.5(5)	3.39(1)
		bridging[a]	2.09(1), 2.18(1)	1.18(1)	1.57(1)	178.8(9)			
4	$[Ni(L^1)(NCS)_2]_2$ (**6**)	terminal[a]							3.03(1)
		bridging[a]							
5	$[Ni_2(L^2)(AcO)_2(NCS)^2(MeOH)]$ (**5**)	terminal[a]	2.105(6)					88.1(2)	2.993(1)
		bridging[a]	2.131(5), 2.172(5)						
6	$[Ni_2(L^2)(NCS)^3(MeOH)]$ (**5**)	terminal[a]	2.008(7)						3.142(2)
		bridging[a]	2.039(7), 2.170(6)						
7	$[Ni(L^2)(NCS)_3(urea)]$ (**5**)	terminal[a]	2.002(6)						3.155(2)
		bridging[a]	2.077(5), 2.197(5)						
8	$[Ni_2(S\text{-}dept)_2(NCS)_4]$ (present work)	terminal[a]	2.018(9)	1.15(1)	1.63(1)	179.2(10)	170.8(8)	96.9(8)	3.316(5)
		bridging[a]	2.022(7), 2.396(8)	1.14(1)	1.60(1)	176.1(9)	149.2(8), 113.8(7)		

[a] Average value of M–N (terminal), C–N, C–S, NCS and MNC are given.

had two equal Re–N bonds with Re–Re bond (Table 3). However, Cd^{II} complex contained slightly different M–N bond lengthsand no M–M bond [16]. In the case of Ni^{2+} this type of bonding has been reported for five complexes [17–19] all of them showed bidentate bridging through N of the NCS anion with Ni–Ni distance ranging between 2.993(1) and 3.39(1) Å. In the present complex, the two M–N bond lengths are significantly different from each other and the shorter Ni–N4 distance is comparable to Ni–N5 distance of the terminally bonded NCS anion. Thus the present complex becomes the first example to show maximum asymmetry in bidentate bridging through N atom of the NCS anion. No M–M bonding has been found in the case of any of the Ni^{2+} complexes yet the M–M distance seems to be dependent upon M–N–M (Table 3).

3.2.2. Complex *2*

Crystallization of $[Ni(NCS)_2(O\text{-}deap)(CH_3CN)]\cdot CH_3CN$ by slow evaporation of its saturated solution in acetonitrile at room temperature yields good single crystals. Fig. 3 displays the ORTEP diagram of **2** which crystallizes in $P2_1$ space group with 2 molecules per unit cell. The coordination around the Ni atom can be best described as octahedral as can be ascertained from the bond lengths and angles (Table 2). However, contrary to the expected value in an octahedral geometry, one of the *trans* ligand–metal–ligand angle is not 180° but deviated to a value of 154.3° (O1–Ni1–O2). This apparent deviation from the ideal value may be attributed to the geometrical constraints of O-deap acting as a tridentate meridonal ligand. The two thiocyanate ligands show a marked difference of approach towards the metal coordination polyhedra. While one of the SCN moiety (i.e., S1–C18–N5, Fig. 3) that is placed parallel to O-deap, approaches the metal almost in a nearly linear arrangement (C18–N5–Ni1 = 178°), the other thiocyanate ligand (i.e., S2–C19–N6, Fig. 3) which is approaching orthogonal to the former is substantially deviated from linearity, the C19–N6–Ni1 angle being 162.7°. Nevertheless, their coordinating strengths are almost same as reflected from their almost equal Ni–N bond lengths of 1.995 and 2.043 Å. It is also noteworthy that this type of subtle deviations can modify the geometry around the metal centre. For example, the two five membered rings formed out of the two carbonyl to the metal centre (⩾C=O1···Ni1 and ⩾C=O2···Ni1, Fig. 3) are not placed parallel, but have taken a wedge shape with a wedge angle of 3.7° (angle between the least square planes of these two five membered rings). Similarly, the planar pyridyl moiety is also bent with respect to these rings, the angle between the planes of aromatic pyridyl moiety and the five membered ring involving O1 (i.e., N1, Ni1, O1, C6 and C1) is 11.6° and that with the other ring containing O2 (i.e., N1, Ni1, O2, C11 and C5) is 14.2°. These type of variations, most probably are not only controlled by electronic effects alone, but also

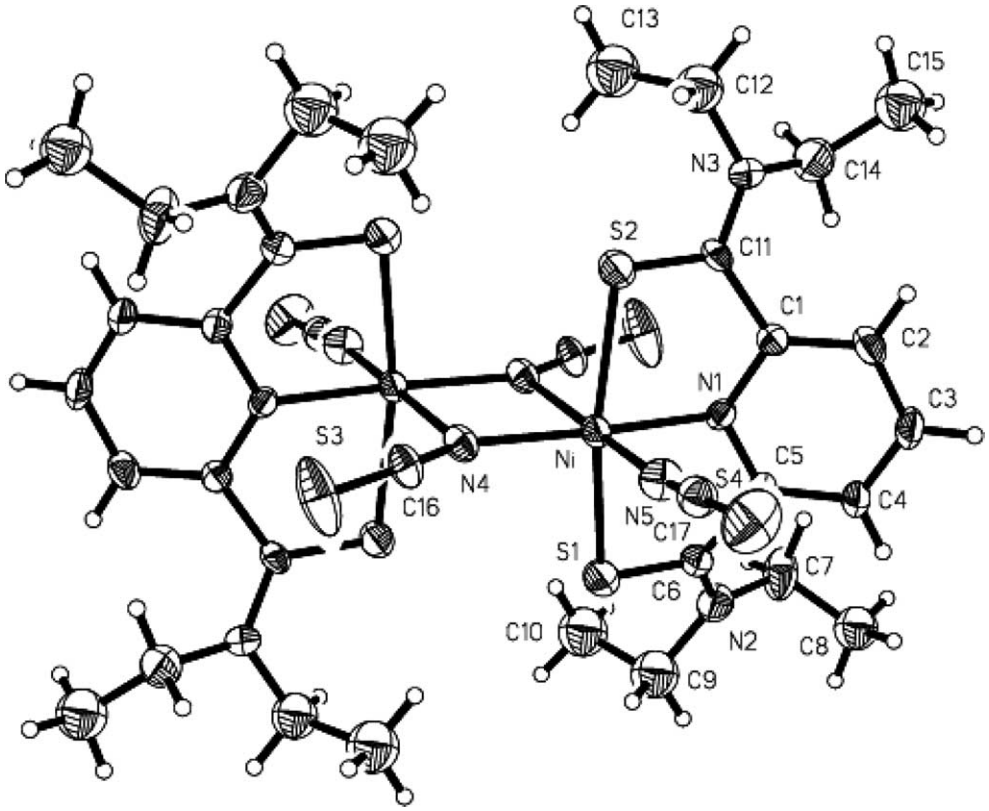

Fig. 2. A perspective view of complex **1** with the atom numbering scheme (thermal ellipsoids are at 50% probability level).

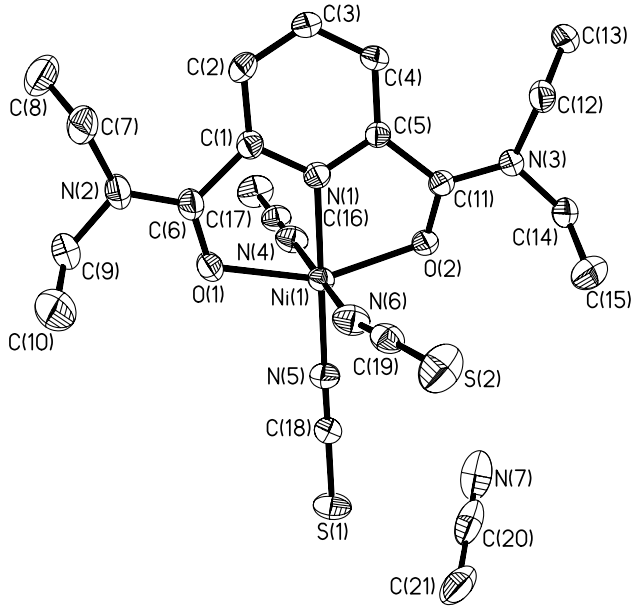

Fig. 3. A perspective view of complex **2** with the atom numbering scheme (thermal ellipsoids are at 50% probability level).

by the subtle steric requirements that are needed for a stable lattice. Such effects which minimize the overall steric congestion are reflected even in the 'coordinating arms' of the ligand. The symmetrically positioned ethyl part of the arms on both sides are placed one 'up' and one 'down' with respect to the meridonal plane of the ligand as evidenced from Fig. 3. The two terminal methyl groups (C10 and C15) that are closer to the coordinating oxygen atoms are 'up' while the other two (C8 and C13) which are away from these oxygen atoms are 'down' (the sense of up and down is with respect to the planar meridonal ligand plane when viewed parallel to Ni(1)–N(1) vector). The sixth coordination of the octahedral geometry is completed by the solvent of crystallization (CH_3CN) itself and its reduced Lewis basicity compared with SCN^- (and hence the weaker coordinating ability) is clear from the higher Ni–N bond length of 2.141 Å. However, the approach towards the metal centre is almost linear, the Ni1–N4–C16 angle being 177.5°.

The role of solvent used for crystallization is twofold in stabilizing the metal ligand complex. Firstly, it completes the coordination around the metal center and imparts stability and secondly, during the packing of molecules in the lattice, the voids generated are filled by these solvent molecules again providing overall stability to the three-dimensional lattice. Packing of this acetonitrile lattice inclusion complex is shown in Fig. 4. Two 'arms' of the neighbouring ligand molecules and the methyl group of the coordinating CH_3CN together generates a cavity and the CH_3CN molecules are occupied in these centres. The stability to this inclusion is imparted through two weak C–H···N interactions of the nitrogen atom of CH_3CN (N7···H12A–

Cl2 = 2.704 and N7···H17C–Cl7 = 2.798 Å) and the other is through a C–H···S interaction of the methyl group of CH_3CN (S1···H21A–C21 = 3.152 Å) and sulphur atom of the thiocyanate moiety. In effect a linear CH_3CN molecule is anchored from both of its terminal ends to the center of the cavity through C–H···N and C–H···S interactions involving the solvent and metal ligand complex. In addition there are three lattice stabilizing C–H···S interactions (involving sulphur atoms of SCN^- moiety) observed in the lattice, S2···H9A–C9 = 2.885, S2···H7A–C7 = 2.922 and S1···H13A–C13 = 3.080 Å.

3.2.3. Complex 3

The structure of **3** obtained after recrystallization in ethanol, is presented in Fig. 5. The coordination around the Ni atom in **3** is also distorted octahedral (Table 2). The difference of 4.3° in the O–Ni–O angle in **2** (154.3°) from **3** (150.0°) shows that O-deap ligand can adopt to subtle geometrical requirements during the complex formation. However, to meet the steric demands, the pyridyl part of O-deap has to undergo a substantial bend from the mean plane of the two five membered rings formed out of the coordination to Ni atom (Fig. 5), the angle being 21.8°. It is interesting that the same deviation in **2** is only 12.7 showing that change in the coordination from acetonitrile to ethanol can have profound influence in the overall topology of the metal ligand complex. As in **2**, the two five membered rings are also wedge shaped, infact the wedge angle has increased to 5.5°. The approach of the two thiocyanate ligands is very similar to that of **2**, the one in the plane of the ligand is linearly placed with respect to the metal (C16–N4–Ni1 = 174.2°), whereas the other orthogonally placed one makes an angle of 163.2° (C17–N5–Ni1). The coordinating arms of the ligand have a very similar up and down conformation as in **2**.

Participation of the amide nitrogen in the coordination process through amide resonance is evident from the very planar nature of N atoms of both **2** and **3** (sum of the angles around nitrogen is 359.8° (**2**) and 359.6° (**3**), respectively). This type of resonance would facilitate more charge on the carbonyl oxygens for better participation in metal–ligand coordination. It is noteworthy that the major difference in the octahedral coordination of Ni in **2** and **3** is that the acetonitrile in **2** is replaced by an ethanol molecule in **3**. Out of the six octahedral metal–ligand bonds in **2**, it is the Ni–N(acetonitrile) that is the longest (2.141 Å, Table 2). However, since enhanced Lewis basicity can be expected for the oxygen atom of ethanol (than that of the nitrogen atom of CH_3CN), the Ni–O(ethanol) is no longer the highest and is reduced to 2.078 Å. In fact it is the shortest among the three Ni–O bonds in **3** (Table 2).

We hypothesised that the sixth coordination of compound **2** can be replaced, if a solvent of similar size (but with equal or higher Lewis basicity) can be used for crystallization. Another motivation was to examine the role

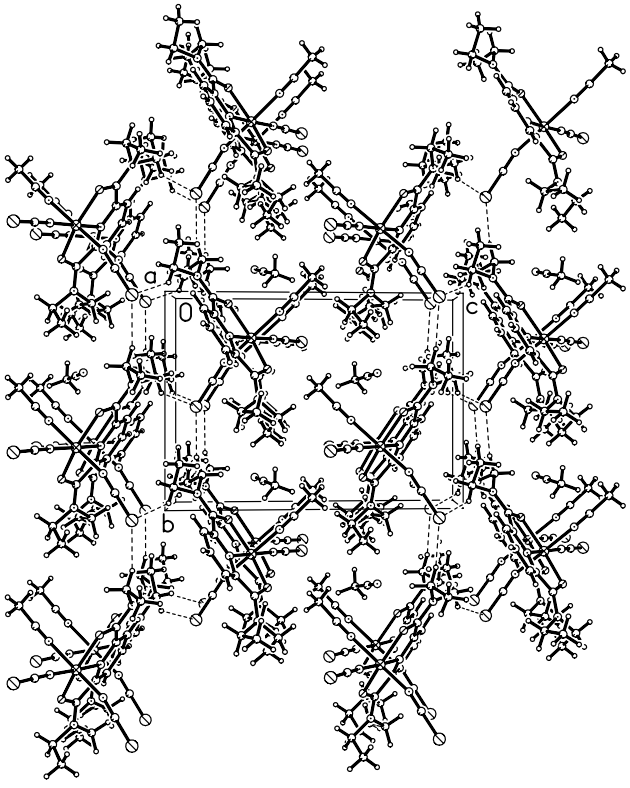

Fig. 4. Packing of complex **2** viewed perpendicular to the *bc* plane.Note the occpancy of solvent acetonitrile (right to the middle of unit cell) in the cavity formed from the arms of the ligand and the methyl group of coordinated CH_3CN. The lattice stabilizing C–H···S interactions are shown by dotted lines.

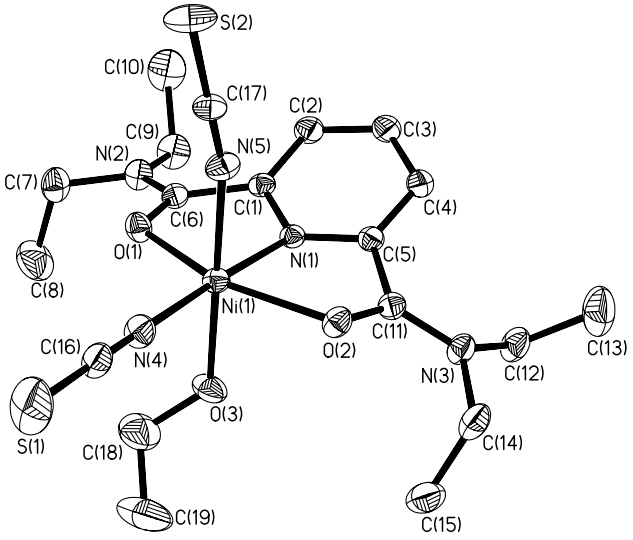

Fig. 5. A perspective view of complex **3** with the atom numbering scheme (thermal ellipsoids are at 50% probability level).

of solvent in stabilizing the three-dimensional lattice, after all, does the solvent play a deciding role in the lattice formation? If so, the compound would display polymorphism, which is of contemporary interest [25]. Ethanol was conceived as appropriate solvent as it satisfies both the condition of size and Lewis basicity. Gratifyingly, compound **3** was successfully crystallized from absolute ethanol with an ethanol occupying the sixth position in the octahedral coordination. But interestingly no solvent of crystallization was included in the lattice and the molecular packing is significantly different from that of **2**. A packing diagram viewed down the *ab* plane is shown in Fig. 6.

In the lattice, one of the thiocyanate groups (i.e., S1–C16–N4) is involved in a lattice stabilizing C–H···S interaction (C10–H10A···S1 = 2.835 Å) whereas the other one (i.e., S2–C17–N5) is hydrogen bonded to the hydrogen atom of the coordinated ethanol (O3–H3A···S2 = 2.431 Å) through a O–H···S hydrogen bond. Thus, as in **2** both the thiocyanate groups are involved in S–H···O/C interactions. In addition, the hydrogen atom at the para position of the pyridyl moiety also takes part in a C–H···O hydrogen bond with one of the carbonyl oxygen atoms (C3–H3B···O2 = 2.448 Å). Thus, our initial hypothesis of obtaining a complex in which the replacement of an acetonitrile with ethanol was realized, but the lack of inclusion of ethanol as a solvent of crystallization amply displays the complex interplay of weak interactions in stabilizing the three-dimensional lattice of these molecules. These observations show that, at molecular level certain predictability can be realized, but the nature of molecular packing is still a complex process to comprehend and indeed it is one of the challenges in crystal engineering [26].

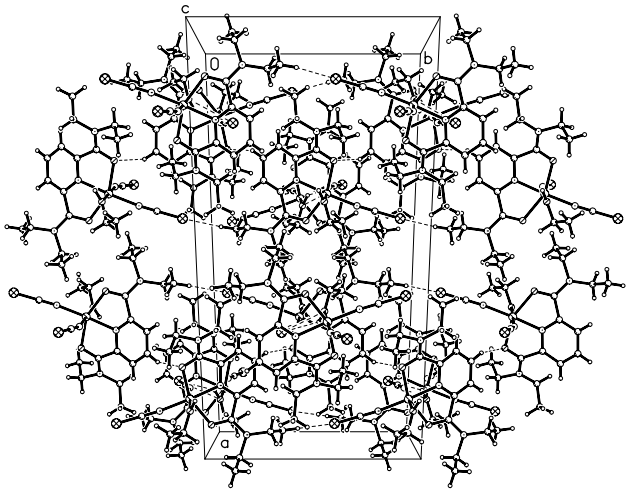

Fig. 6. Packing of complex **3** viewed perpendicular to the *ab* plane. The lattice stabilizing C–H···S interactions are shown by dotted lines.

Acknowledgements

We sincerely thank Professor Rabindranath Mukherjee for his kind help with low temperature magnetic susceptibility measurements on complex **1**. A.K. is grateful to CSIR, New Delhi, India for senior research fellowship.

Appendix A. Supplementary material

Supplementary data associated with this article can be found, in the online version at doi:10.1016/j.poly.2005.04.006.

References

[1] (a) F.A. Chavez, M.M. Olmstead, P.K. Mascharak, Inorg. Chem. 35 (1996) 1410;
(b) F.A. Chavez, M.M. Olmstead, P.K. Mascharak, Inorg. Chem. 36 (1997) 6323;
(c) D.S. Marlin, M.M. Olmstead, P.K. Mascharak, Inorg. Chem. 38 (1999) 3258;
(d) J.C. Noveron, M.M. Olmstead, P.K. Mascharak, J. Am. Chem. Soc. 121 (1999) 3553;
(e) D.S. Marlin, M.M. Olmstead, P.K. Mascharak, Inorg. Chim. Acta 297 (2000) 106;
(f) D.S. Marlin, M.M. Olmstead, P.K. Mascharak, J. Mol. Struct. 554 (2000) 211;
(g) J.C. Noveron, M.M. Olmstead, P.K. Mascharak, J. Am. Chem. Soc. 123 (2001) 3247;
(h) D.S. Marlin, M.M. Olmstead, P.K. Mascharak, Inorg. Chem. 40 (2001) 7003.
[2] (a) A.K. Singh, V. Balamurugan, R. Mukherjee, Inorg. Chem. 42 (2003) 6497;
(b) M. Ray, D. Ghosh, Z. Shirin, R. Mukherjee, Inorg. Chem. 36 (1997) 3568;
(c) A.K. Patra, R. Mukherjee, Inorg. Chem. 38 (1999) 1388.
[3] D.S. Marlin, P.K. Mascharak, Chem. Soc. Rev. 29 (2000) 69.
[4] (a) S.M. Redmore, C.E.F. Rickard, S.J. Webb, L.J. Wright, Inorg. Chem. 36 (1997) 4743;
(b) T. Yano, R. Tanaka, T. Nishioka, L. Kinoshita, K. Isobe, L.J. Wright, T. Collins, J. Chem. Commun. (2002) 1396.
[5] T. Kawamoto, B.S. Hammes, R. Ostrander, A.L. Rheingold, A.S. Borovik, Inorg. Chem. 37 (1998) 3424.
[6] (a) F. Renaud, C. Piguet, G. Bernardinelli, J.C.G. Bunzli, G. Hopfgartner, Chem. Eur. J. 3 (1997) 1646;
(b) T. Le Borgne, J.M. Benech, S. Floquet, G. Bernardinelli, C. Aliprandini, P. Bettens, C. Piguet, J. Chem. Soc., Dalton Trans. (2003) 3856.
[7] (a) P. Kapoor, A. Kumar, J. Nistandra, P. Venugopalan, Transition Met. Chem. 25 (2000) 465;
(b) R. Kapoor, A. Kataria, P. Kapoor, P. Venugopalan, Transition Met. Chem. 29 (2004) 425;
(c) P. Kapoor, A. Kataria, P. Venugopalan, R. Kapoor, M. Corbella, M. Rodriguez, M. Romero, A. Llobet, Inorg. Chem. 43 (2004) 6699.
[8] (a) J.G.H. De Preez, B. van Brecht, J.F. de Wet, J. Koorts, Inorg. Nucl. Chem. Lett. 10 (1974) 935;
(b) J.G.H. de Preez, B.J.A.M. van Brecht, Inorg. Chim. Acta 162 (1989) 49.

[9] (a) J. Garcia-Lozano, M.A. Martinez-Lorento, E. Escriva, R. Ballesteros, Synth. React. Inorg. Met. Org. Chem. 24 (1994) 365;
(b) J. Garcia-Lozano, L. Soto, J.V. Folgado, E. Escriva, Polyhedron 15 (1996) 4003.
[10] Siemens, XSCANS, X-ray Single Crystal System, Version 2.1, Siemens Analytical X-ray Instruments Inc., Madison, WI, USA, 1994.
[11] G.M. Sheldrick, SHELXTL-PC, Release 5.03, Siemens Analytical X-ray Instruments Inc., Madison, WI, USA 1995.
[12] M. Nardelli, PARST, Comput. Chem. (1983) 95.
[13] W.J. Geary, Coord. Chem. Rev. 7 (1971) 81.
[14] (a) P.C.H. Mitchell, R.J.P. Williams, J. Chem. Soc. (1960) 1912;
(b) J. Lewis, R.S. Nyholm, P.W. Smith, J. Chem. Soc. (1961) 4590;
(c) J.L. Burmeister, Coord. Chem. Rev. 1 (1966) 205;
(d) J.L. Burmeister, Coord. Chem. Rev. 3 (1968) 225.
[15] F.A. Cotton, A. Davison, W.H. Ilsley, H.S. Trop, Inorg. Chem. 18 (10) (1979) 2719.
[16] L.R. Groeneveld, G. Vos, G.C. Verschoor, J. Reedijk, J. Chem. Soc., Chem. Commun. (1982) 620.
[17] T. Koga, H. Furutachi, T. Nakamuura, N. Fukita, M. Ohba, K. Takahashi, H. Okawa, Inorg. Chem. 37 (1998) 989.
[18] (a) P.A. Harding, K. Henrick, L.F. Lindoy, M. McPartlin, P.A. Tasker, J. Chem. Soc., Chem. Commun. (1983) 1300;
(b) K.R. Adam, A.J. Leong, L.F. Lindoy, B.J. McCool, A. Ekstrom, I. Liepa, P.A. Harding, K. Henrick, M. McPartlin, P.A. Tasker, J. Chem. Soc., Dalton Trans. 11 (1987) 2537.
[19] G.A. van Albada, R.A.G. de Graff, J.G. Haasnoot, J. Reedijk, Inorg. Chem. 23 (1984) 1404.
[20] D.-T. Wu, C.-S. Chung, Inorg. Chem. 25 (1986) 3584, and references therein.
[21] J.A.A. Mokuolu, J.C. Speakman, Acta Crystallogr., Sect. B 31 (1975) 172, and references therein.
[22] L. Pauling, The Nature of Chemical Bond, Cornell University Press, Ithaca, NY, 1960.
[23] (a) D.V. Naik, W.R. Scheidt, Inorg. Chem. 12 (1973) 272;
(b) M.G.B. Drew, A.H. bin Othman, S.G. McFall, P.D.A. Mcllroy, S.M. Nelson, J. Chem. Soc., Dalton Trans. (1977) 438.
[24] (a) S.E. Livingstone, Quart. Rev. Chem. Soc. 19 (1965) 386;
(b) M.G.B. Drew, A.H. bin Othman, S.M. Nelson, J. Chem. Soc., Dalton Trans. (1976) 1394.
[25] For a special issue on polymorphism in crystals: fundamentals, prediction and industrial practice, see: in: R.D. Rogers (Ed.), Cryst. Growth Des. 3 (6) (2003).
[26] (a) G.R. Desiraju, Crystal engineering: the design of organic solids, Elsevier, Amsterdam, 1989;
(b) J.-M. Lehn, Supramolecular Chemistry: Concepts and Perspectives, VCH, Weinheim, 1995;
(c) D.S. Lawerence, T. Jiang, M. Levett, Chem. Rev. 95 (1995) 2229.